Water Science & Technology

Water Science & Technology Vol 88 No 5, 1317 doi: 10.2166/wst.2023.269

Selective electrodialysis process for the recovery of potassium from multicomponent solution systems

Xiaofu Guo[a,b,c], Lei Xiang[a], Mengmeng Sun[a,b,c], Shizhao Wang[a,b,c], Zhiyong Ji[a,b,c], Jingtao Bi[a,b,c] and Yingying Zhao[a,b,c,d,*]

[a] School of Chemical Engineering and Technology, Hebei University of Technology, No. 8, Guangrong Road, Hongqiao District, Tianjin 300130, China
[b] Engineering Research Center of Seawater Utilization of Ministry of Education, No. 8, Guangrong Road, Hongqiao District, Tianjin 300130, China
[c] Hebei Collaborative Innovation Center of Modern Marine Chemical Technology, No. 8, Guangrong Road, Hongqiao District, Tianjin 300130, China
[d] Tianjin Key Laboratory of Chemical Process Safety, Tianjin 300130, China
*Corresponding author. E-mail: luckyzhaoyy@126.com

ABSTRACT

Selective electrodialysis is a promising approach to recovering K^+ from complex coexisting ionic systems. In this study, the effects of current density, the concentration of K^+ and Mg^{2+}, as well as the operating temperature on the separation process of K^+ and Mg^{2+} were explored to investigate the competitive migration of mono- and multivalent ions, offering a guide for the design of selective electrodialysis process, and therefore obtain the desired aqueous solutions containing K^+ and Mg^{2+}. The results show that ion concentration played a critical role in determining the selectivity of separation between K^+ and Mg^{2+}. High concentrations of K^+ and Mg^{2+} led to a decrease in selectivity but the effect of concentration of K^+ on selectivity was more pronounced. Although higher current density increased the flux of ions, their impact on separation selectivity was minimal. Furthermore, higher temperature increased the flux of ions but resulted in a decrease of K^+ proportion in the solution. Overall, this study provides good guidance for studying the competitive migration of mono- and multivalent ions and the high-value recycling of potassium resources.

Key words: competitive migrations, selective electrodialysis, separation of K^+ and Mg^{2+}

HIGHLIGHTS

- Selective electrodialysis was used for the separation of potassium and magnesium ions.
- The main factors affecting the competitive migration of mono- and multivalent ions were systematically explored.
- Potassium resource was efficiently recovered by selective electrodialysis.

GRAPHICAL ABSTRACT

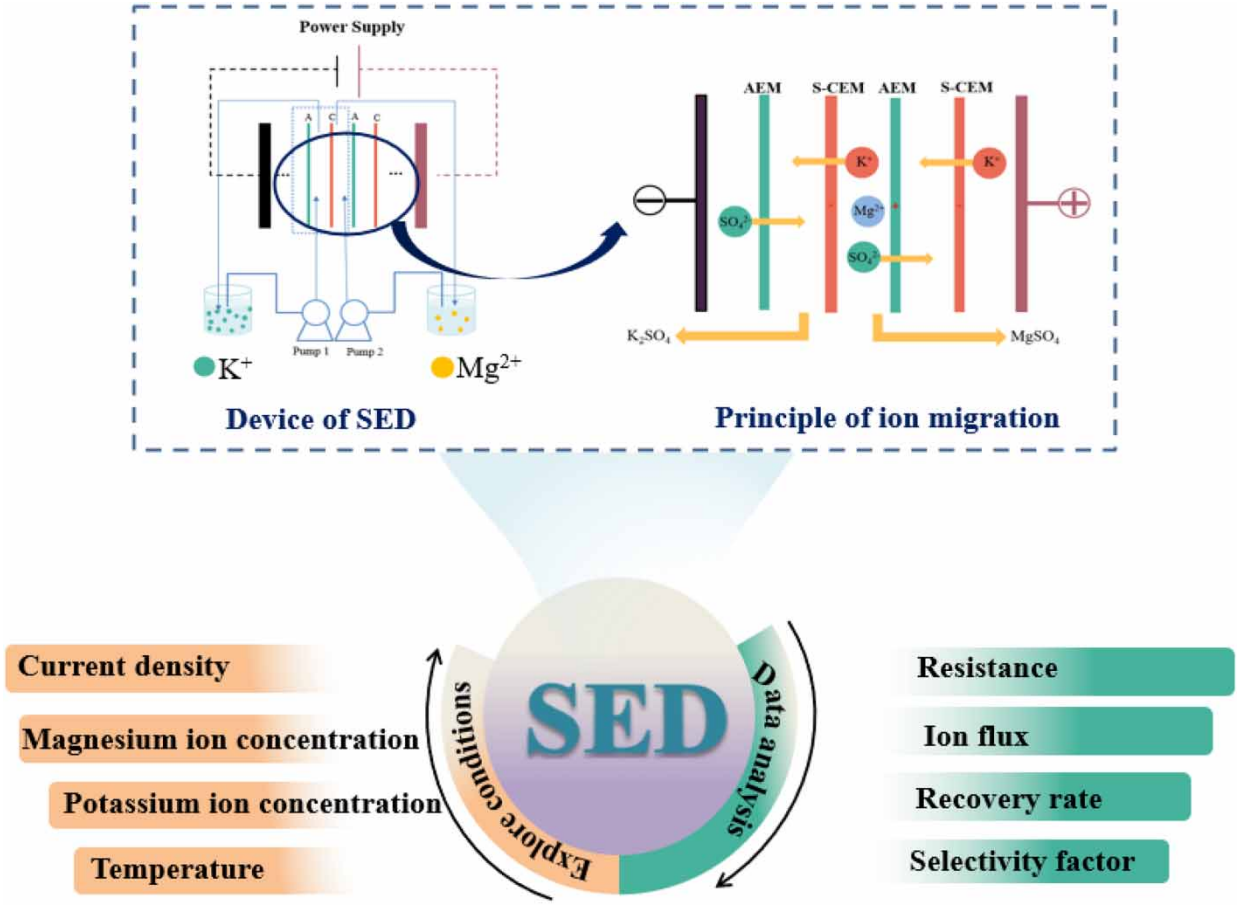

1. INTRODUCTION

Potassium fertilizer is a strategic resource indispensable for food grain production, while nearly half of China's potassium fertilizer is imported due to the shortage of potassium resources (Chen *et al.* 2020). How to effectively recover and utilize the potassium resources and hence accelerate the development of agriculture in China is an important issue (Li 2013). It was reported that most potassium resources are extracted from soluble potash ores and Salt Lake brines (Ciceri *et al.* 2015; Hongwen *et al.* 2015). Recently, crop straw has been regarded as a promising raw material to recover potassium since potassium fertilizer applied to crops can also be a raw material for obtaining potassium resources (Hou *et al.* 2021; Ru Fang *et al.* 2022; Wang *et al.* 2023), which provides benefits in terms of potassium life cycle and sustainable development (Yakovleva *et al.* 2021; Song *et al.* 2022). In addition, wine lees and food waste can also be critical raw materials of potassium resources extraction (Madejón *et al.* 2001), whereas the obtained potassium resource usually contain other coexisting ions, typically Mg^{2+}.

Separation of monovalent K^+ and multivalent Mg^{2+} is crucial to recover potassium resources with high purity. Commonly, mono- and multivalent ions can be separated by adsorption (Guo *et al.* 2020; Zhang *et al.* 2021a), membrane technology (Li *et al.* 2022; Liu *et al.* 2023a) and precipitation (Jumaeri *et al.* 2021; Liu *et al.* 2023b). However, adsorption is limited by the adsorption capacity. Traditional membrane technology typically uses nanofiltration membranes, which requires severe operating conditions but possesses somewhat lower selectivity. Post-treatment of the precipitation method will be relatively troublesome. To overcome the limitations facing the aforementioned methods, electrodialysis technology is developed as a new type of electrically driven membrane separation technology to separate ions. It can deal with solutions in large quantities without investing large amounts of chemical reagents. It is, therefore, used in several industries for ion separation (Abou-Shady 2017; Sedighi *et al.* 2023). Selective electrodialysis (SED) is a unique technique that can separate mono- and

multivalent ions. The monovalent ion exchange membrane used in SED enables the smooth passage of monovalent ions but blocks the migration of multivalent ions. Anna Siekierka and Fatma Yalcinkaya (Siekierka & Yalcinkaya 2022) developed a monovalent ion exchange membrane with high cobalt ion selectivity. They ultimately enabled cobalt the removal of cobalt from multicomponent solutions up to 91% with a separation factor of 5.6 for lithium and cobalt. Zhang *et al.* (Zhang *et al.* 2021b) developed a selective electrodialysis process in the feed-discharge mode that allows continuous lithium extraction from brines with low Li^+ concentrations to obtain high-purity lithium carbonate after SED. The use of SED is becoming more widespread as the need to extract high-value products from wastewater increases. Many studies have been reported on the extraction of lithium from lithium-magnesium coexistence systems, however, limited studies have been performed on K^+/Mg^{2+} separation. Considering the separation of K^+/Mg^{2+} is demanded in a wide range of application scenarios (Hancer & Miller 2000; Duan *et al.* 2006; Widyatmoko & Burgman 2006), we developed an SED process to efficiently recover K^+ from K_2SO_4/Mg_2SO_4 solution. The effects of current density, potassium/magnesium ion concentrations and their ratios, as well as temperature, on the recovery rate of K^+ and separation selectivity of K^+/Mg^{2+} were systematically investigated, with the influencing mechanisms analyzed by examining the migration pathways of target (K^+) and impurity (Mg^{2+}) ions.

2. EXPERIMENTAL SECTION

2.1. Materials and equipment

The reagents used in the experiments were analytically pure, and the water used was deionized water produced in the laboratory. A five-compartment polytetrafluoroethylene (PTFE) electrodialysis test tank was used for the experiment. The selective cation exchange membrane was purchased from Astom of Japan, and the anion exchange membrane (AEM) was purchased from YDS Environmental Equipment Co., Ltd (Langfang, China).

2.2. Electrodialysis device

In this experiment, an electrodialysis tank with an effective membrane area of 3 cm × 5 cm was used. The electrodialysis device consists of a concentration tank, a dilution tank, an auxiliary chamber tank, an electrode liquid tank, a direct-current (DC) power supply, and a membrane stack. The schematic diagram of the device is shown in Figure 1(a) where the cation and

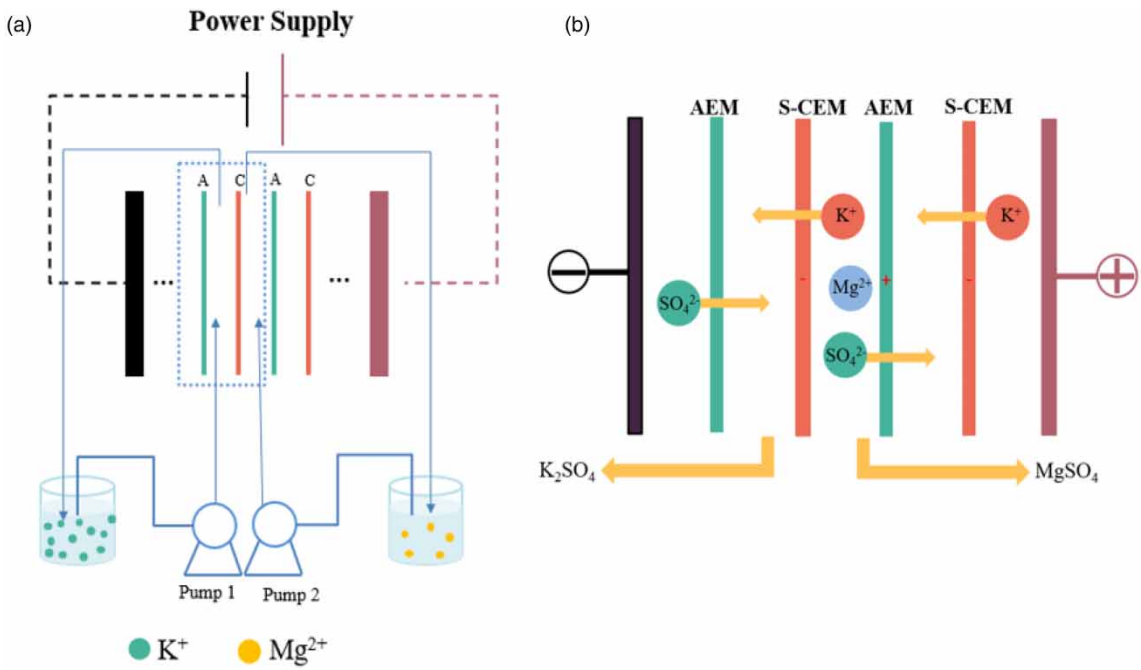

Figure 1 | Schematic diagrams of the experimental device and process: (a) experimental device of SED and (b) principle of ion migration mechanism.

anion exchange membranes were denoted by C and A, respectively, and the experimental schematic diagram is shown in Figure 1(b).

2.3. Experimental procedures

Both the concentration and auxiliary chambers were configured with 0.1 L K_2SO_4 solution, with an initial concentration being 0.1 mol/L. 0.1 L of solution containing both K_2SO_4 and $MgSO_4$ with a certain concentration were filled in the desalination chamber. 0.2 L of K_2SO_4 solution with an initial concentration of 0.5 mol/L served as the electrode solution. The solution from each chamber was pumped into the membrane stack to circulate the solution and to make the solution more uniform in each chamber. The experimental process was carried out for 120 min, during which the solution samples in the concentration and desalination chambers were taken out every 20 min. Each group of experiments was performed three times, and the average value of the concentration of K^+ and Mg^{2+} was taken.

To investigate the effects of current density, potassium ion concentration, magnesium ion concentration, and temperature on ion migration, experiments were conducted under different conditions in this study, and the parameters of the experimental conditions are shown in Table 1.

2.4. Ion concentration analysis methods

The concentration of K^+ was determined by sodium tetraphenylborate-quaternary ammonium titration and atomic absorption spectrophotometer (TAS-990F). The concentration analysis of Mg^{2+} was performed by an automatic potentiometric titration analyzer (Titration Excellence T7, Mettle Toledo, Switzerland) and atomic absorption spectrophotometer. The analytical methods and standards for each ion concentration are shown in Table 2.

Table 1 | Operating conditions of SED experiment

NO.	Current density (A/m^2)	Mg^{2+} in the desalination chamber (mol/L)	K^+ in the desalination chamber (mol/L)	*T* (°C)
1	100	0.50	0.20	25
2	150	0.50	0.20	25
3	200	0.50	0.20	25
4	250	0.50	0.20	25
5	200	0.29	0.20	25
6	200	0.20	0.20	25
7	200	0.15	0.20	25
8	200	0.13	0.20	25
9	200	0.50	0.35	25
10	200	0.50	0.50	25
11	200	0.50	0.65	25
12	200	0.50	0.85	25
13	200	0.50	0.65	20
14	200	0.50	0.65	30
15	200	0.50	0.65	35

Table 2 | Analytical methods and basis for each ion

Ion type	Content (g/L)	Methods	Reference
K^+	>2	NaTPB-ACQ titration method	(Guo *et al.* 2015)
	<2	Atomic absorption spectrophotometer (TAS-990F)	(Schiopu *et al.* 2009)
Mg^{2+}	>1	EDTA titration method	(Ji *et al.* 2017; Chen *et al.* 2021)
	<1	Atomic absorption spectrophotometer (TAS-990F)	(Schiopu *et al.* 2009)

2.5. Data analysis

2.5.1. Resistance

The resistance (Ω) refers to the ratio of voltage to current on both sides of the film stack, as shown in Equation (1).

$$R = \frac{U}{I} \tag{1}$$

where U (V) represents the voltage on both sides of the membrane stack and I (A) denotes the current flow.

2.5.2. Ion flux

Ion flux J (mol·m^{-2}·h^{-1}) refers to the average migration number of ion through a unit membrane area in a given time, as shown in Equation (2).

$$J = \frac{(C_{K^+} - C_0) \times V}{N \times S \times \Delta t} \tag{2}$$

where C_{K^+} (mol/L) is the K^+ concentration in the concentrate, C_0 (mol/L) is the K^+ initial concentration in concentration chamber. V (L) is the solution volume, N denotes the number of replicate units. S is the effective area of each ion exchange membrane, and in this work, it is 0.0015 m^2. Δt (min) is the time interval.

2.5.3. Recovery rate

Recovery rate (%) of K^+ was calculated by Equation (3):

$$R_{K^+} = \frac{C(K^+)_{nt} \times V_{nt} - C(K^+)_{n0} \times V_{n0}}{C(K^+)_{d0} \times V_{d0}} \tag{3}$$

where $C(K^+)_{nt}$ (mol/L) is the concentration of K^+ in the concentration chamber at time t, V_{nt} (L) is the volume of solution in the concentration chamber at time t, $C(K^+)_{n0}$ and $C(K^+)_{d0}$ (mol/L) indicate the initial concentrations of K^+ in the concentration and desalination chambers, respectively. V_{n0} and V_{d0} (L) are the initial volumes of solution in the concentration and desalination chambers, respectively.

2.5.4. Selectivity factor

The selectivity factor indicates the amount ratio of K^+ migration to Mg^{2+} migration during the experiment, as shown in Equation (4).

$$S_{K^+/Mg^{2+}} = \frac{(C(K^+)_{nt} \times V_{nt} - C(K^+)_{n0} - V_{n0})/(C(Mg^{2+})_{nt} \times V_{nt} - C(Mg^{2+})_{n0} - V_{n0})}{C(K^+)_{d0}/C(Mg^{2+})_{d0}} \tag{4}$$

where $C(K^+)_{nt}$, $C(Mg^{2+})_{nt}$ (mol/L) are the concentrations of K^+ and Mg^{2+} in the concentration chamber at time t, $C(K^+)_{n0}$, $C(Mg^{2+})_{n0}$ (mol/L) are the initial concentrations of K^+ and Mg^{2+} in the concentration chamber, and V_{nt}, V_{n0} (L) are the volumes of solutions in the concentration chamber at time t and at the initial time.

3. RESULTS AND DISCUSSION

The conditions affecting the competitive migration of coexisting ions are complex, and the following experiments were conducted to investigate the effects of various factors on the separation performance of K^+/Mg^{2+}.

3.1. Effects of current density

Current density determines the migration ability of positively and negatively charged particles (Ozkul *et al.* 2023). This section, hence, examines the effect of current density (100, 150, 200, and 250 A/m^2) on electrodialysis, and all the studied current densities are within the range of the limiting current density (Min *et al.* 2021).

As shown in Figure 2(a) and 2(b), the concentration of K^+ in the concentration chamber increases, while the concentration of K^+ in the desalination chamber decreases continuously during the experiment with time. At the same time, the high

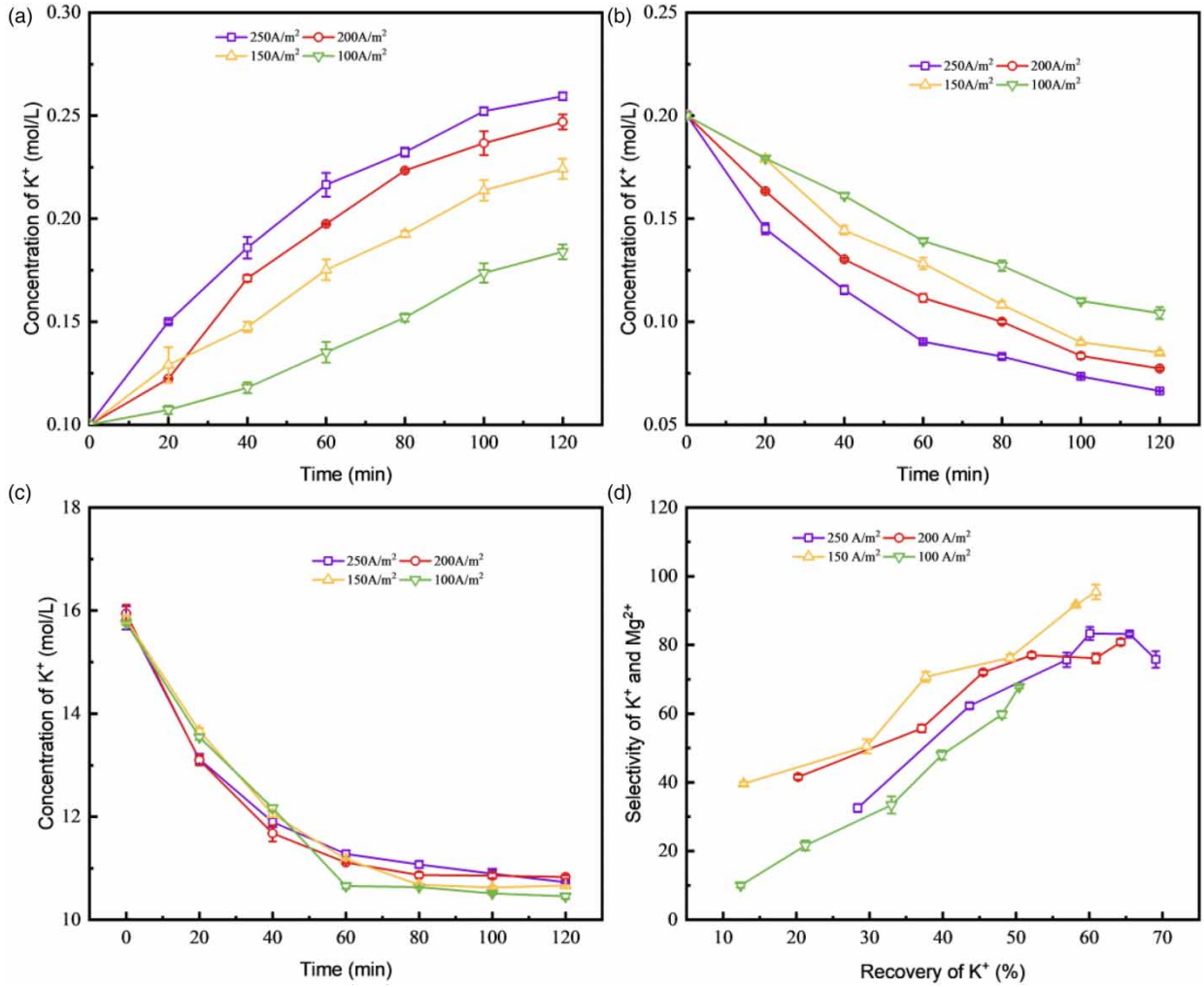

Figure 2 | Effects of current density on (a) concentration of K^+ in the concentration chamber; (b) concentration of K^+ in the desalination chamber; (c) membrane stack resistance; and (d) variation of $S_{K^+/Mg^{2+}}$ versus K^+ recovery rate.

current density can accelerate the migration of K^+ to the concentration chamber since the increased current density could increase the mass transfer driving force and separation efficiency of ions (Szczygiełda *et al.* 2017). In the scenarios of 100 and 150 A/m^2, the concentration of K^+ in the concentration chamber increases almost linearly while it linearly decreases in the desalination chamber. However, when the current density is 200 or 250 A/m^2, the concentration curve of K^+ in the concentration chamber first approaches linear increase and then tends to be flat. This may be because the intermittent experiment does not involve feed replenishment, and thus in the later stage of the investigation, K^+ in the desalination chamber almost entirely migrates and there is no enough K^+ to migrate to the boundary layer (Kim *et al.* 2011, 2012), resulting in a slow increase in the concentration of K^+ migrating to the concentration chamber in the later part of the experiment. As the current density increased, the K^+ migration rate accelerated, as shown in Figure 2(a) and 2(b).

As shown in Figure 2(c), the initial membrane stack resistance is the highest since at this time, the solution in each chamber is heterogeneous and the ion concentrations in the concentration chamber are low. K^+ gradually migrates to the concentration chamber as the experiment proceeds, and the solutions in each chamber tend to be homogeneous in their own uniform. This leads to a better conductivity and decreased resistance of the solutions. In addition, the migration amount of K^+ at low current density is less than that at high current density. Therefore, in the later stage of the SED, the ion concentration in the desalination chamber increases with the decreasing current density as evidenced by Figure 2(b), leading to the lowest resistance at 100 A/m^2 (Szczygiełda & Prochaska 2017). The variation of $S_{K^+/Mg^{2+}}$ with recovery rate of K^+ at different

current densities is shown in Figure 2(d). The overall upward trend of $S_{K^+/Mg^{2+}}$ with the increase of rate is due to the relatively high selectivity of the membrane. It is known from Figure 2(a) that the higher the current density is, the more K^+ will migrate across the membrane. At the same time, the impurity ion Mg^{2+} will also migrate faster with the increased electric field driving force. The selectivity is highest at a current density of 150 A/m^2, followed by current densities of 200 and 250 A/m^2. Although low current density can retard the leak of Mg^{2+}, the mobility of K^+ decreases at low current densities (Jaroszek *et al.* 2016). Therefore, as the current density decreases, $S_{K^+/Mg^{2+}}$ becomes smaller.

As shown in Figure 3, current density has a significant impact on the average ion flux, and fluxes of K^+ and Mg^{2+} increase with the increase of current density. When the current density was increased from 100 to 150 A/m^2, the flux of K^+ increased significantly, while the flux of Mg^{2+} increased slightly. This is because monovalent ions have higher diffusion coefficients than divalent ions (Ozkul *et al.* 2023; Sireci *et al.* 2023). When the current density increases 200–250 A/m^2, the flux of K^+ increases by about 28% and the flux of Mg^{2+} increases by about 35%. This may be because both ions are subjected to an increased migration driving force with the increase of current density. Whereas Mg^{2+} carries more charge than K^+, therefore, more Mg^{2+} leaked into the concentration chamber under the effect of a larger electric field force.

It can be found that low current density leads to a decrease in ion migration rate and efficiency, while high current density can accelerate ion migration but lead to a relatively high leak of Mg^{2+}. At 200 A/m^2, more potassium ions were migrated, and the leakage of Mg^{2+} was relatively small. This leaded to an effective improvement in selectivity while ensuring efficiency, therefore, a current density of 200 A/m^2 was chosen for the subsequent experiments.

3.2. Effects of magnesium ion concentration

It is well documented that initial ion concentration significantly impacts ion migration (Zhu *et al.* 2020). In this section, the competitive migration mechanism of ions was explored by analyzing the variation of concentration of K^+, the variation of a flux of Mg^{2+}, and the variation of $S_{K^+/Mg^{2+}}$ with recovery rate at different Mg^{2+} concentrations.

From Figure 4(a), it can be seen that the migration of K^+ toward the concentration chamber is influenced by Mg^{2+} concentration. This is because there is a competitive relationship between the migrations of Mg^{2+} and K^+ (Yang *et al.* 2022). When the ratio of K^+/Mg^{2+} is greater than 1, the initial concentration of Mg^{2+} in the desalination chamber is relatively low, and its effect on K^+ migration is slight. However, when K^+/Mg^{2+} is less than 1, the increase of Mg^{2+} concentration results in the reduction of K^+ migration amount from the desalination chamber to the concentration chamber. That is because Mg^{2+} in high concentration may form a double layer at the interface of the cation exchange membrane and the solution. This reduces

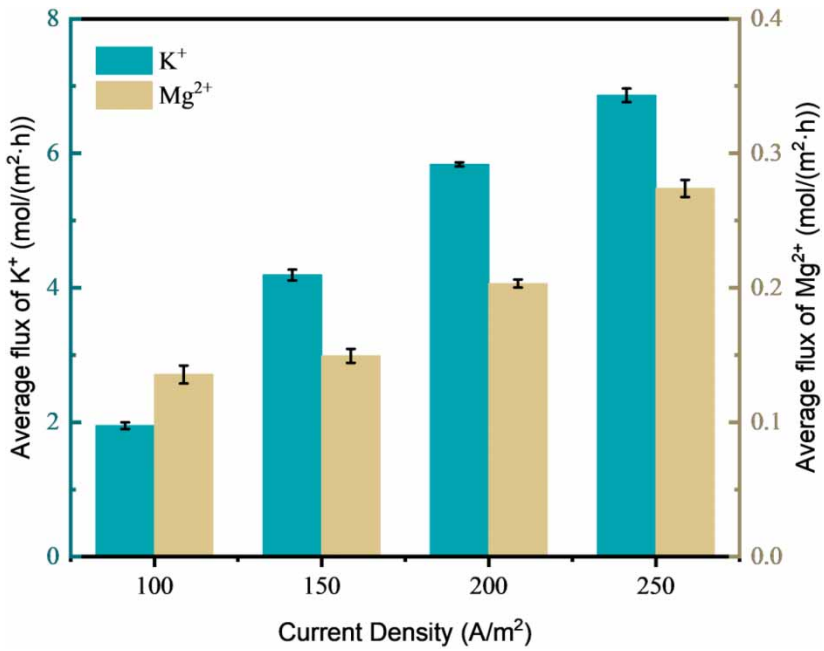

Figure 3 | Variation of average ion fluxes of K^+ and Mg^{2+} versus current density.

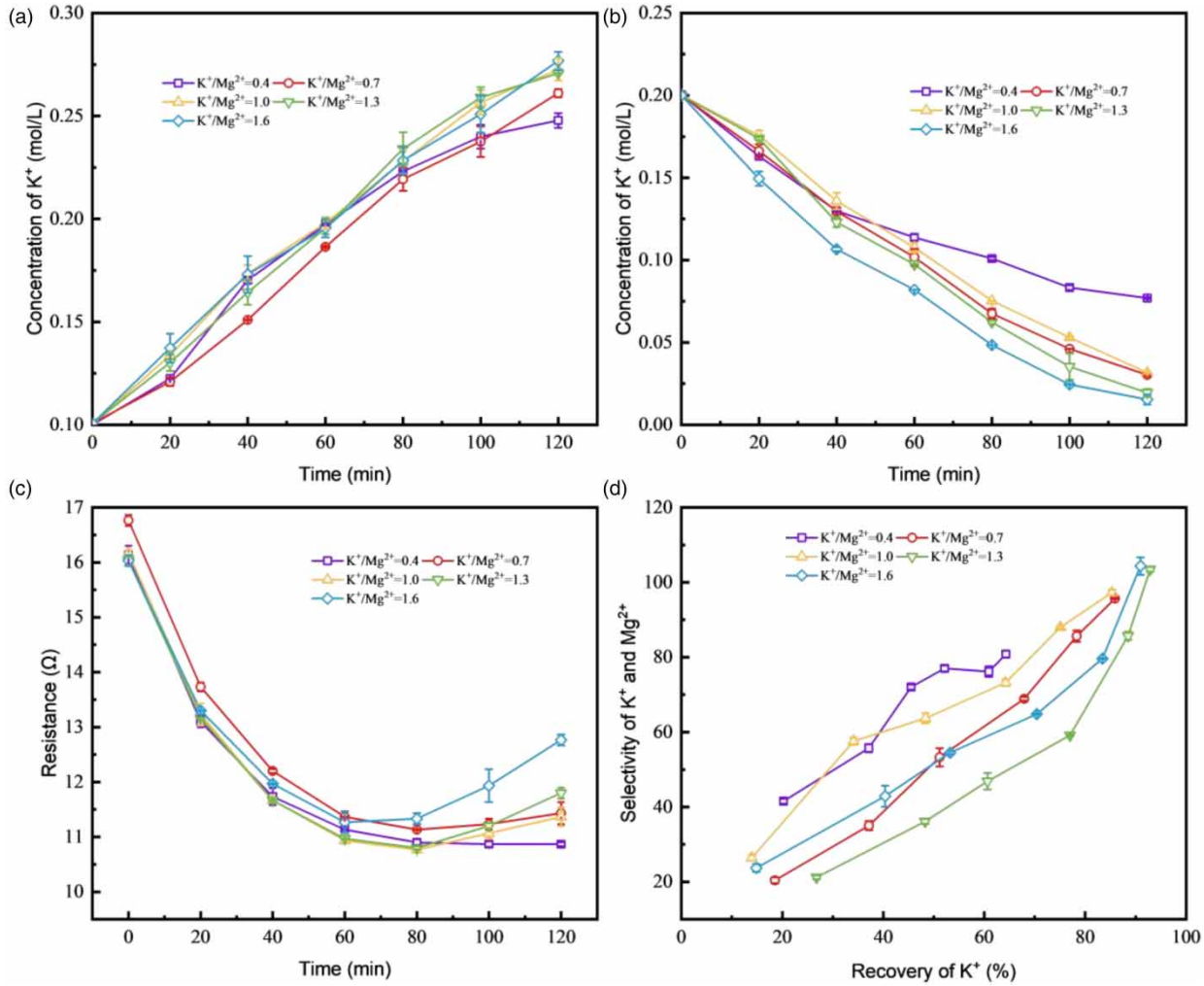

Figure 4 | Effects of magnesium ion concentration on (a) concentration of K^+ in the concentration chamber; (b) concentration of K^+ in the desalination chamber; (c) membrane stack resistance; (d) variation of $S_{K^+/Mg^{2+}}$ with K^+ recovery rate.

the active sites for K^+ transfer (Weisbrod *et al.* 2016) and forms a positively charged interfacial layer (Nie *et al.* 2017; Wang *et al.* 2022), leading to charge repulsion between the CEM and K^+. Moreover, the increasing Mg^{2+} concentration increases the solution viscosity of the desalination chamber, leading to a decrease in the diffusion coefficient of ions (Weisbrod *et al.* 2016). Therefore, when the concentration of Mg^{2+} is high, the migration of K^+ is inhibited. Figure 4(b) shows the change of K^+ concentration in the desalination chamber, which corresponds to that in Figure 4(a).

Figure 4(c) shows the effects of Mg^{2+} concentration on the resistance. It is regarded that a single valence selective ion exchange membrane has a high migration resistance to Mg^{2+}. Therefore, Mg^{2+} will accumulate on the membrane surface, forming a stronger positive layer and a greater repulsive force against K^+. At the same time, the amount of K^+ that can migrate from the desalination compartment to concentration chamber decreases, thus the membrane stack resistance will have a slight upward trend after the initial decrease, as shown in Figure 4(c).

The $S_{K^+/Mg^{2+}}$ and recovery rate of K^+ were plotted in Figure 4(d). When $K^+/Mg^{2+} = 0.4$, Mg^{2+} with high concentration results in great migration competition with K^+ and lower recovery rates. When $K^+/Mg^{2+} = 0.7$ and 1.0, the final values of $S_{K^+/Mg^{2+}}$ and recovery rate are similar but higher than that at $K^+/Mg^{2+} = 0.4$. When $K^+/Mg^{2+} = 1.3$ and 1.6, the concentrations of Mg^{2+} are similar and relatively low, therefore, both the recovery rate and $S_{K^+/Mg^{2+}}$ are improved.

It can be seen from Figure 5 that the concentration of Mg^{2+} has opposite effects on K^+ and Mg^{2+} fluxes. The average ion flux of K^+ decreases as the concentration of Mg^{2+} in the initial raw material solution increases. The Mg^{2+} leakage flux

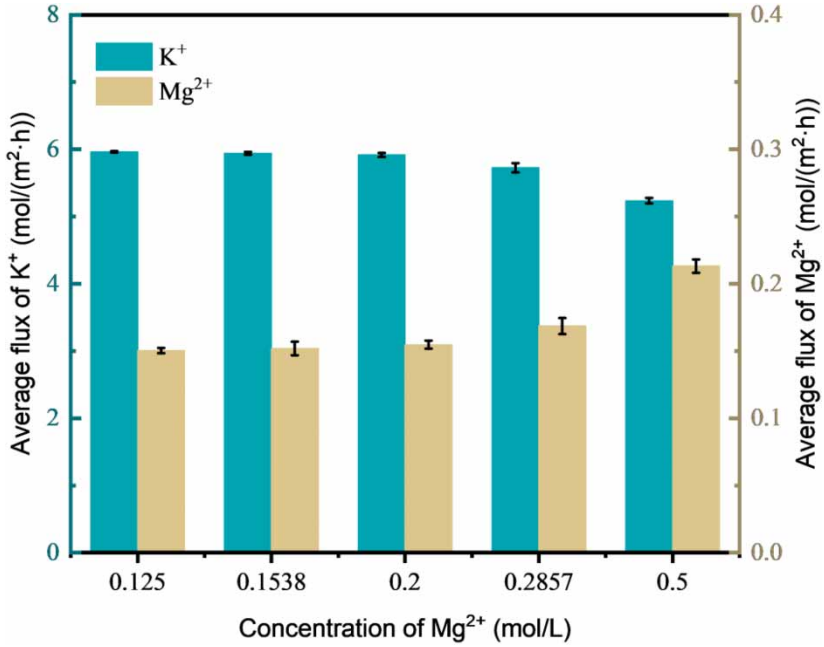

Figure 5 | Variation of average ion fluxes of K^+ and Mg^{2+} versus concentration of Mg^{2+}.

increases with the increase of Mg^{2+} concentration. When the Mg^{2+} concentrations are at low levels (0.125, 0.1538, and 0.20 mol/L), its influence on the ion fluxes is slight. While the concentration of Mg^{2+} increases to higher concentrations (0.2857 and 0.50 mol/L), there is an obvious decline in the K^+ flux but an increase in Mg^{2+} flux was observed. When the Mg^{2+} concentration is low, the average flux of K^+ migrating to the concentrate compartment remains almost unchanged, and the increase of Mg^{2+} leakage flux is unobvious. However, when Mg^{2+} concentration was increased to a higher concentration, the K^+ flux showed a significant decrease, which may be due to factors such as solution viscosity and double layer. And the leakage of Mg^{2+} also showed a significant increase.

In summary, changes in Mg^{2+} concentration can affect the migration of both ions. The greater the concentration of impurity ions is, the greater the effects on the migration of the target ions are. Therefore, the concentration of Mg^{2+} was chosen as 0.5 mol/L for the following experimental investigation.

3.3. Effects of potassium ion concentration

Competitive migration between ions is influenced by the initial concentration of the two competing ions (Ding *et al.* 2021). In this section, the migration patterns of ions under different concentrations of K^+ (0.20, 0.35, 0.50, 0.65, and 0.80 mol/L) were investigated while the Mg^{2+} concentration was kept at 0.50 mol/L.

As shown in Figure 6(a), the final concentration of K^+ in the concentrator increases as the initial K^+ concentration in the desalination chamber was increased. When $K^+/Mg^{2+} = 0.4$, the concentration of K^+ in the concentrator increases slightly after 80 min. That is because the concentration of K^+ in the desalination chamber is low at this time, resulting in a low level of transmembrane migration of K^+. When $K^+/Mg^{2+} \geq 1.0$, the K^+ concentration in the concentrator no longer increases significantly with the increased K^+ concentration in the desalination chamber, as shown in Figure 6(a) and 6(b).

As shown in Figure 6(c), the membrane stack resistance decreases as the experiment proceeded. Higher K^+/Mg^{2+} ratio leads to higher conductivity and lower membrane stack resistance. It may be because the high concentration of K^+ increases the concentration gradient on both sides of the ion exchange membrane and enhances the migration tendency of ions. Therefore, ions are more likely to pass through the ion exchange membrane, leading to a decrease in membrane resistance. At the same time, the migration of the impurity ion Mg^{2+} is inhibited as the concentration of the target ion K^+ increases, which reduces the contribution of Mg^{2+} to the resistance of the ion exchange membrane, resulting in a decrease in resistance. Figure 6(d) shows that both $S_{K^+/Mg^{2+}}$ and recovery rate gradually decreases with the increase of K^+/Mg^{2+} ratio. This is because the increase of the initial K^+ concentration cannot result in equivalent increase in K^+ flux due to the constant membrane separation ability and electric field driving force.

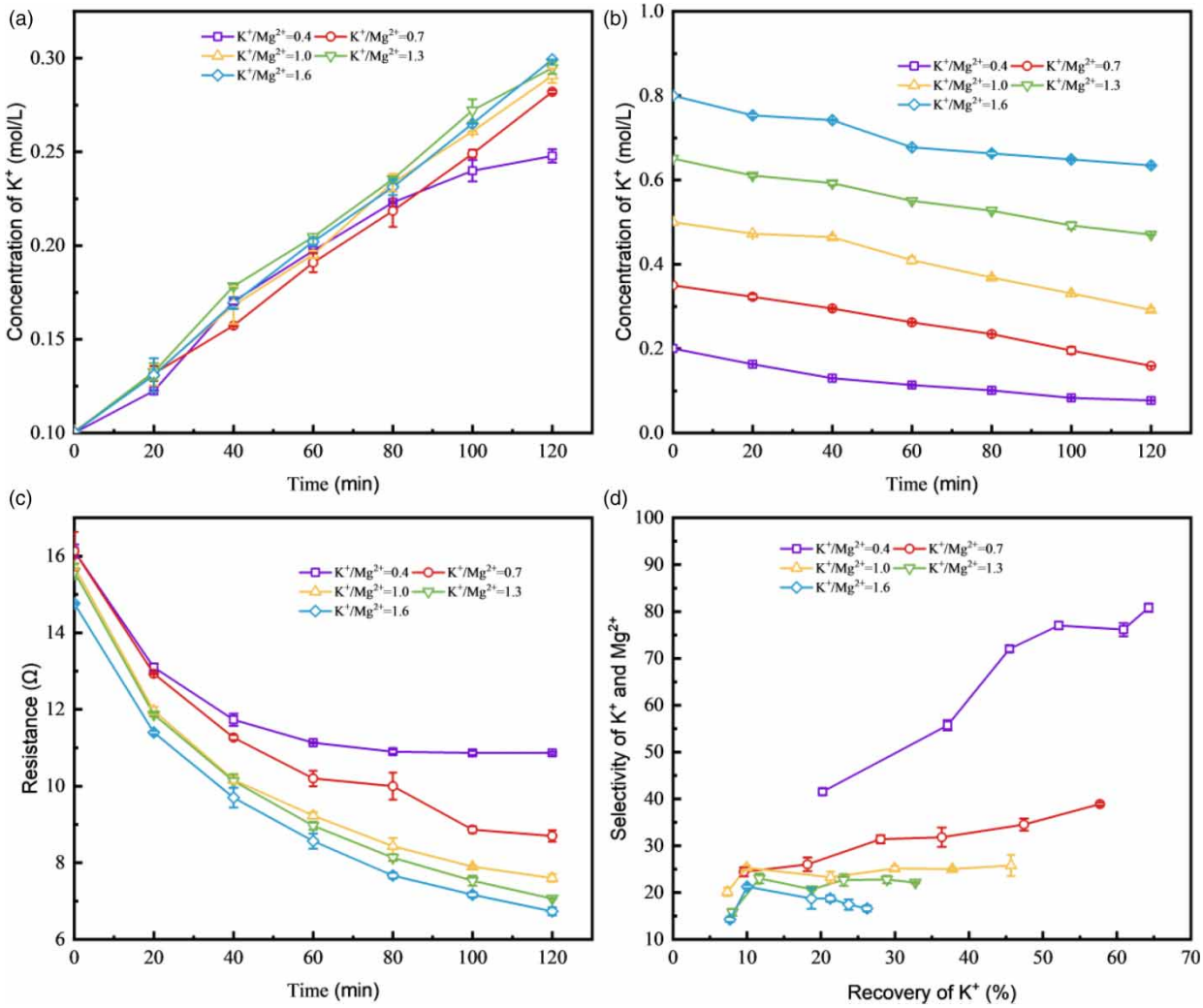

Figure 6 | Effects of potassium ion concentration on (a) concentration of K^+ in the concentration chamber; (b) concentration of K^+ in the desalination chamber; (c) membrane stack resistance; (d) variation of $S_{K^+/Mg^{2+}}$ with K^+ recovery rate.

Average fluxes of K^+ and Mg^{2+} under different K^+ concentrations were depicted in Figure 7. As the initial concentration of K^+ increases, the flux of K^+ transferred to the concentration chamber shows an increasing trend, while the flux of Mg^{2+} almost shows a continuous decreasing trend.

Whereas when the initial concentrations of K^+ are 0.65 and 0.80 mol/L, the K^+ fluxes are almost the same. This is probably because the processing capacity of the ion exchange membrane is limited, and the solution viscosity increases with the increase of ion concentration (Weisbrod *et al.* 2016), which is unfavorable for the migration of target ions. The flux of Mg^{2+} leaked into the concentration chamber shows a continuous decreasing trend with the increase of the initial concentration of K^+. The increase in the migration of the target ion K^+ decreases the leakage of the impurity ion Mg^{2+}, which is due to the competitive migration of ions and the ion exchange capacity is fixed within a certain range.

In summary, a high initial concentration of K^+ can induce a larger K^+ flux while suppress the leakage of Mg^{2+} toward concentration chamber. Therefore, we chose to conduct further experimental investigations with the initial concentration of K^+ of being kept at 0.65 mol/L.

3.4. Effects of temperature

Lower temperatures can reduce the conductivity and diffusion coefficient of the solution, leading to a slower migration rate of ions. Moreover, excessively low temperatures may make the ion exchange membrane become hard or brittle, shortening its

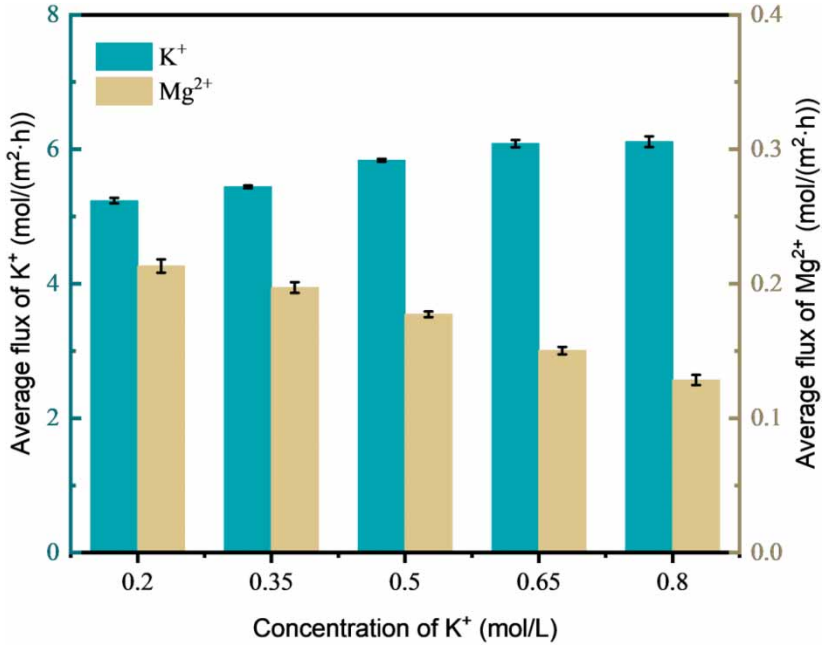

Figure 7 | Variation of average ion fluxes of K^+ and Mg^{2+} versus concentration of K^+.

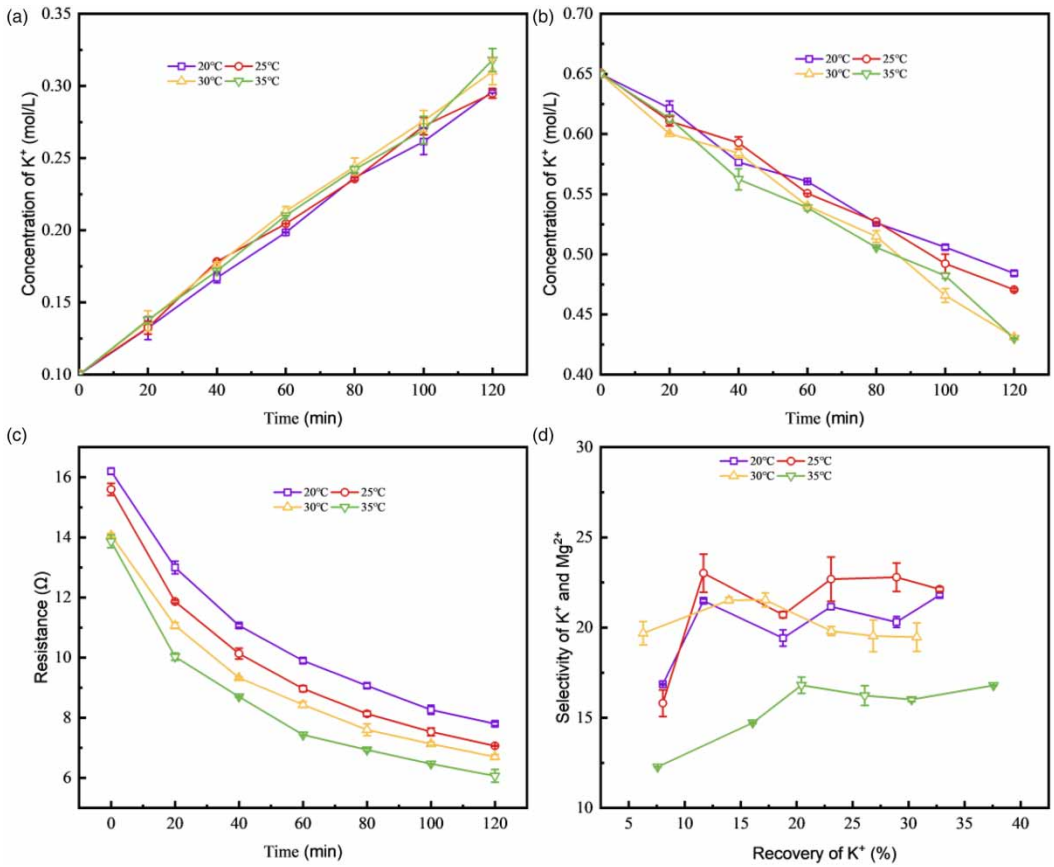

Figure 8 | Effects of temperature on (a) concentration of K^+ in the concentration chamber; (b) concentration of K^+ in the desalination chamber; (c) membrane stack resistance; and (d) variation of $S_{K^+/Mg^{2+}}$ with K^+ recovery rate.

service life. Higher temperatures can lead to the failure of the ion exchange membrane. The ion exchange membrane is usually made of polymer materials, and an increase in temperature can reduce the thermal stability of polymer materials (Zhang *et al.* 2019; Zheng *et al.* 2022), thereby affecting the separation performance of the ion exchange membrane. Therefore, the solution temperature should be controlled below 40 °C, and the impact of temperature on ion migration was shown in Figure 8.

As can be seen from Figure 8(a), the increase in temperature has a promoting effect on the migration of K^+ to the concentration chamber, and the concentration of K^+ in the concentration chamber shows an increasing trend with the increase of temperature, which is consistent with the variation trend shown in Figure 8(b). This is mainly because the viscosity of the solution decreases with the increase in temperature. Also, the increased molecular kinetic energy at high temperature accelerates the ion migration rate. Figure 8(c) shows that the resistance decreases as the temperature increases. This can be explained by the effects of temperature on diffusion, the hydration layer, and the pore size of the membrane. High temperature increases the diffusion coefficient and accelerates the ion migration rate, thus resulting in a faster decrease in resistance. In addition, ions migrate across the membrane in a hydrated form (Chen *et al.* 2013). The increase in temperature is more likely to break the hydration layer, making it easier for ions to migrate. Also, high temperature can increase the pore size of the membrane, which can improve the mass transfer rate. Although the increase of temperature accelerated the migration of the target ion K^+, it also aggravated the leakage of Mg^{2+}. As shown in Figure 8(d), when the temperature is low (20 and 25 °C) the leakage amount of Mg^{2+} is small, resulting in high selectivity. At 30 and 35 °C, although the migration amount of K^+ is higher when compared with that at low temperatures, the facilitation effects of high temperature on the migration of Mg^{2+} is higher than that on K^+ migration (Benneker *et al.* 2018), which decreased the selectivity.

Average fluxes of K^+/Mg^{2+} from desalination chamber to concentration chamber at different temperatures were depicted in Figure 9. Both the average fluxes of the target ion K^+ and the impurity ion Mg^{2+} show increasing trends with the increase of temperature. The fluxes of K^+ and Mg^{2+} increased slightly when the temperature was increased from 20 to 30 °C. At 35, the K^+ flux decreases slightly compared to 30 °C, while the Mg^{2+} flux increases obviously, which may be due to the higher transportability of Mg^{2+} at higher temperatures. The ion fluxes increased with increasing temperature, which shows that Mg^{2+} is more influenced by temperature and the migration of K^+ is limited by the increase of Mg^{2+} migration.

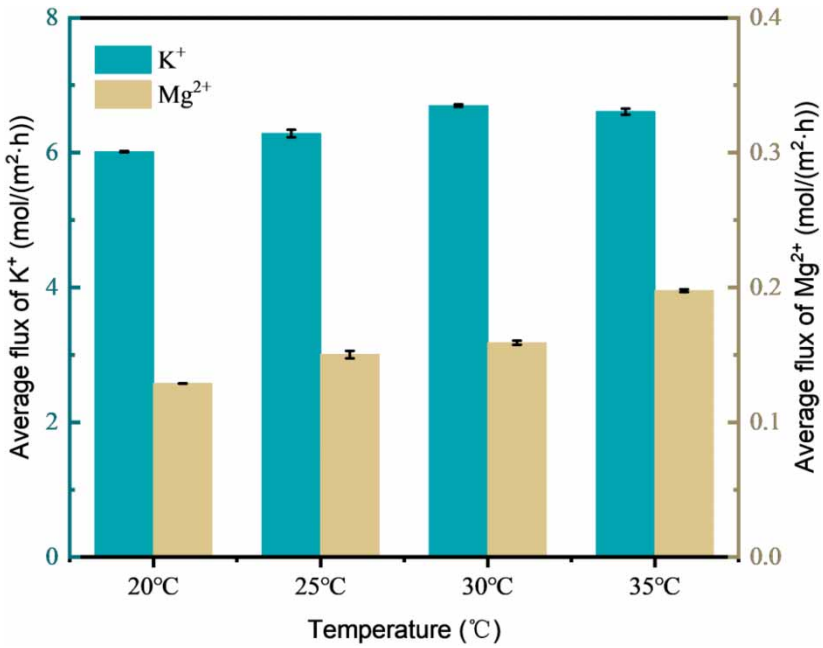

Figure 9 | Variation of average ion fluxes of K^+ and Mg^{2+} versus temperature.

4. CONCLUSIONS

In order to effectively achieve the selective separation of mono- and multivalent ions, in this study, the effects of current density, target ion concentration, impurity ion concentration, and temperature on the competitive migration of K^+ and Mg^{2+} were investigated. It was found that both the migration fluxes of K^+ and Mg^{2+} increased with the increasing current density. A noticeable competitive migration between K^+ and Mg^{2+} was demonstrated: an increase of the initial concentration of K^+ favors the migration of itself while inhibiting the leakage of Mg^{2+}. While the increase of initial concentration of Mg^{2+} also causes an inhibitory effect on the migration of K^+. There is an optimal temperature at which the highest $S_{K^+/Mg^{2+}}$ can be obtained. The final results show that the current density has the greatest effect on the ion flux, and the target ion concentration has the greatest effect on the selectivity of mono- and multivalent ions. However, a combination of $S_{K^+/Mg^{2+}}$ and ion fluxes, the final choice of current density was 200 A/m^2 and the initial concentration of target ion K^+ was 0.65 mol/L and the initial concentration of Mg^{2+} was 0.5 mol/L. This work provides a good guide for the recovery of K^+ by SED from complex systems and the competitive migration of mono- and multivalent ions.

ACKNOWLEDGEMENTS

This work is funded by Tianjin Science and Technology Project (20JCZDJC00450), Natural Science Foundation of Hebei Province (B2020202029), Central Guidance on Local Science and Technology Development Fund of Hebei Province (226Z3102G), Fundamental Research Funds of Hebei University of Technology (JBKYTD2001).

DECLARATION OF COMPETING INTEREST

The authors declared that there is no conflict of interest.

DATA AVAILABILITY STATEMENT

All relevant data are included in the paper or its Supplementary Information.

CONFLICT OF INTEREST

The authors declare there is no conflict.

REFERENCES

Abou-Shady, A. 2017 Recycling of polluted wastewater for agriculture purpose using electrodialysis: perspective for large scale application. *Chemical Engineering Journal* **323**, 1–18.

Benneker, A. M., Klomp, J., Lammertink, R. G. H. & Wood, J. A. 2018 Influence of temperature gradients on mono- and divalent ion transport in electrodialysis at limiting currents. *Desalination* **443**, 62–69.

Chen, S., Luo, H., Hou, Y., Liu, G., Zhang, R. & Qin, B. 2013 Comparison of the removal of monovalent and divalent cations in the microbial desalination cell. *Frontiers of Environmental Science & Engineering* **9** (2), 317–323.

Chen, X., Li, T., Lu, D., Cheng, L., Zhou, J. & Wang, H. 2020 Estimation of soil available potassium in Chinese agricultural fields using a modified sodium tetraphenyl boron method. *Land Degradation & Development* **31** (14), 1737–1748.

Chen, T., Zhao, Y., Zhao, Y., Xie, Y., Ji, Z., Guo, X., Zhao, Y. & Yuan, J. 2021 Competitive ion migration and process optimization of carbon sequestration and seawater decalcification in a bipolar electrodialysis process. *ACS Sustainable Chemistry & Engineering* **9** (25), 8372–8382.

Ciceri, D., Manning, D. A. & Allanore, A. 2015 Historical and technical developments of potassium resources. *Science of the Total Environment* **502**, 590–601.

Ding, R., Ding, Z., Chen, X., Fu, J., Zhou, Z., Chen, X., Zheng, X., Jin, Y. & Chen, R. 2021 Integration of electrodialysis and Donnan dialysis for the selective separation of ammonium from high-salinity wastewater. *Chemical Engineering Journal* **405**, 127001.

Duan, Z., Sun, R., Zhu, C. & Chou, I. M. 2006 An improved model for the calculation of CO_2 solubility in aqueous solutions containing Na^+, K^+, Ca^{2+}, Mg^{2+}, Cl^-, and SO_4^{2-}. *Marine Chemistry* **98** (2–4), 131–139.

Guo, X.-F., Ji, Z.-Y., Yuan, J.-S., Zhao, Y.-Y. & Liu, J. 2015 Recovery of K^+ from concentrates from brackish and seawater desalination with modified clinoptilolite. *Desalination and Water Treatment* **57** (15), 6829–6837.

Guo, X.-F., Li, D., Liu, J.-L., Wang, Z.-R., Wang, J., Zhao, Y.-Y. & Yuan, J.-S. 2020 Separation of sodium and potassium using adsorption–elution/crystallization scheme from bittern. *Chemical Engineering Research and Design* **161**, 72–81.

Hancer, M. & Miller, J. D. 2000 The flotation chemistry of potassium double salts: schoenite, kainite, and carnallite. *Minerals Engineering* **13** (14–15), 1483–1493.

Hongwen, M. A., Jing, Y., Shuangqing, S. U., Meitang, L. I. U., Hong, Z., Yingbin, W., Hongbin, Q. I., Pan, Z. & Wengui, Y. A. O. 2015 20 years advances in preparation of potassium salts from potassic rocks: a review. *Acta Geologica Sinica – English Edition* **89** (6), 2058–2071.

Hou, Y., Xu, X., Kong, L., Zhang, L. & Wang, L. 2021 The combination of straw return and appropriate K fertilizer amounts enhances both soil health and rice yield in Northeast China. *Agronomy Journal* **113** (6), 5424–5435.

Jaroszek, H., Lis, A. & Dydo, P. 2016 Transport of impurities and water during potassium nitrate synthesis by electrodialysis metathesis. *Separation and Purification Technology* **158**, 87–93.

Ji, Z.-Y., Chen, Q.-B., Yuan, J.-S., Liu, J., Zhao, Y.-Y. & Feng, W.-X. 2017 Preliminary study on recovering lithium from high Mg^{2+}/Li^{+} ratio brines by electrodialysis. *Separation and Purification Technology* **172**, 168–177.

Jumaeri, Mahatmanti, F. W., Rahayu, E. F., Qoyyima, D. & Ningrum, A. N. K. (2021). Recovery of high purity sodium chloride from seawater bittern by precipitation-evaporation method. *Journal of Physics: Conference Series* **1918** (3).

Kim, Y., Walker, W. S. & Lawler, D. F. 2011 Electrodialysis with spacers: effects of variation and correlation of boundary layer thickness. *Desalination* **274** (1–3), 54–63.

Kim, Y., Walker, W. S. & Lawler, D. F. 2012 Competitive separation of di- vs. mono-valent cations in electrodialysis: effects of the boundary layer properties. *Water Research* **46** (7), 2042–2056.

Li, Z. S. 2013 Analysis of potash resource situations in China and development of Yiliping Saline Lake in Qinghai Province. *Advanced Materials Research* **734–737**, 282–285.

Li, Y., Wang, S., Wu, W., Yu, H., Che, R., Kang, G. & Cao, Y. 2022 Fabrication of positively charged nanofiltration membrane with uniform charge distribution by reversed interfacial polymerization for Mg^{2+}/Li^{+} separation. *Journal of Membrane Science* **659**, 120809.

Liu, X., Feng, Y., Ni, Y., Peng, H., Li, S. & Zhao, Q. 2023a High-permeance Mg^{2+}/Li^{+} separation nanofiltration membranes intensified by quadruple imidazolium salts. *Journal of Membrane Science* **667**, 121178.

Liu, X., Zhang, H., Zhang, X., Yang, Y., Yang, C., Zhao, P. & Dong, Y. 2023b Chloride removal from flue gas desulfurization wastewater through Friedel's salt precipitation method: a review. *Science of the Total Environment* **862**, 160906.

Madejón, E., López, R., Murillo, J. M. & Cabrera, F. 2001 Agricultural use of three (sugar-beet) vinasse composts: effect on crops and chemical properties of a Cambisol soil in the Guadalquivir river valley (SW Spain). *Agriculture, Ecosystems & Environment* **84** (1), 55–65.

Min, K. J., Kim, J. H. & Park, K. Y. 2021 Characteristics of heavy metal separation and determination of limiting current density in a pilot-scale electrodialysis process for plating wastewater treatment. *Science of the Total Environment* **757**, 143762.

Nie, X.-Y., Sun, S.-Y., Sun, Z., Song, X. & Yu, J.-G. 2017 Ion-fractionation of lithium ions from magnesium ions by electrodialysis using monovalent selective ion-exchange membranes. *Desalination* **403**, 128–135.

Ozkul, S., van Daal, J. J., Kuipers, N. J. M., Bisselink, R. J. M., Bruning, H., Dykstra, J. E. & Rijnaarts, H. H. M. 2023 Transport mechanisms in electrodialysis: the effect on selective ion transport in multi-ionic solutions. *Journal of Membrane Science* **665**, 121114.

Ru Fang, Y., Zhang, S., Zhou, Z., Shi, W. & Hui Xie, G. 2022 Sustainable development in China: valuation of bioenergy potential and CO_2 reduction from crop straw. *Applied Energy* **322**, 119439.

Schiopu, P., Iancu, O., Panait, C., Schiopu, P., Cristea, I., Caruntu, G., Manea, A., Voinea, V., Grosu, N. & Craciun, A. 2009 Atomic absorption spectrophotometry for the analysis of metal contents in tobacco samples. In: *Advanced Topics in Optoelectronics, Microelectronics, and Nanotechnologies IV* **7297**, 117–120.

Sedighi, M., Behvand Usefi, M. M., Ismail, A. F. & Ghasemi, M. 2023 Environmental sustainability and ions removal through electrodialysis desalination: operating conditions and process parameters. *Desalination* **549**, 116319.

Siekierka, A. & Yalcinkaya, F. 2022 Selective cobalt-exchange membranes for electrodialysis dedicated for cobalt recovery from lithium, cobalt and nickel solutions. *Separation and Purification Technology* **299**, 121695.

Sireci, E., De Luca, G., Luque Di Salvo, J., Cipollina, A. & Micale, G. 2023 Prediction of equilibrium water uptake and ions diffusivities in ion-exchange membranes combining molecular dynamics and analytical models. *Journal of Membrane Science* **668**, 121283.

Song, X., Geng, Y., Zhang, Y., Zhang, X., Gao, Z. & Li, M. 2022 Dynamic potassium flows analysis in China for 2010–2019. *Resources Policy* **78**, 102803.

Szczygiełda, M. & Prochaska, K. 2017 Alpha-ketoglutaric acid production using electrodialysis with bipolar membrane. *Journal of Membrane Science* **536**, 37–43.

Szczygiełda, M., Antczak, J. & Prochaska, K. 2017 Separation and concentration of succinic acid from post-fermentation broth by bipolar membrane electrodialysis (EDBM). *Separation and Purification Technology* **181**, 53–59.

Wang, W., Sun, J., Zhang, Y., Zhang, Y., Hong, G., Moutloali, R. M., Mamba, B. B., Li, F., Ma, J. & Shao, L. 2022 Mussel-inspired tannic acid/polyethyleneimine assembling positively-charged membranes with excellent cation permselectivity. *Science of the Total Environment* **817**, 153051.

Wang, Y., Liang, B. Q., Bao, H., Chen, Q., Cao, Y. L., He, Y. Q. & Li, L. Z. 2023 Potential of crop straw incorporation for replacing chemical fertilizer and reducing nutrient loss in Sichuan Province, China. *Environmental Pollution* **320**, 121034.

Weisbrod, N., Yechieli, Y., Shandalov, S. & Lensky, N. 2016 On the viscosity of natural hyper-saline solutions and its importance: The Dead Sea brines. *Journal of Hydrology* **532**, 46–51.

Widyatmoko, D. & Burgman, M. A. 2006 Influences of edaphic factors on the distribution and abundance of a rare palm (Cyrtostachys renda) in a peat swamp forest in eastern Sumatra, Indonesia. *Austral Ecology* **31** (8), 964–974.

Yakovleva, N., Chiwona, A. G., Manning, D. A. C. & Heidrich, O. 2021 Circular economy and six approaches to improve potassium life cycle for global crop production. *Resources Policy* **74**, 102426.

Yang, Y., Wang, H., Huang, W., Gao, Y., Li, Z. & Wang, X. 2022 Ion migration during freeze-thaw process: a cryo-desalination experiment of saltwater from southern Xinjiang, China. *Desalination* **544**, 116118.

Zhang, J., Chen, X., Long, R., Si, J., Liu, C. & Ma, S. 2019 Preparation and properties of amphoteric ion exchange membrane for all vanadium redox flow batteries. *Results in Physics* **14**, 102373.

Zhang, S., Ou, R., Ma, H., Lu, J., Banaszak Holl, M. M. & Wang, H. 2021a Thermally regenerable metal-organic framework with high monovalent metal ion selectivity. *Chemical Engineering Journal* **405**, 127037.

Zhang, X.-C., Wang, J., Ji, Z.-Y., Ji, P.-Y., Liu, J., Zhao, Y.-Y., Li, F. & Yuan, J.-S. 2021b Preparation of Li_2CO_3 from high Mg^{2+}/Li^{+} brines based on selective-electrodialysis with feed and bleed mode. *Journal of Environmental Chemical Engineering* **9** (6), 106635.

Zheng, Y., Jin, Y., Zhang, N., Wang, D., Yang, Y., Zhang, M., Wang, G., Qu, W. & Wu, Y. 2022 Preparation and characterization of Ti_3C_2TX MXene/PVDF cation exchange membrane for electrodialysis. *Colloids and Surfaces A: Physicochemical and Engineering Aspects* **650**, 129556.

Zhu, H., Yang, B., Gao, C. & Wu, Y. 2020 Ion transfer modeling based on Nernst–Planck theory for saline water desalination during electrodialysis process. *Asia-Pacific Journal of Chemical Engineering* **15** (2), e2410.

First received 23 June 2023; accepted in revised form 11 August 2023. Available online 24 August 2023